Shap. Mem. Superelasticity
DOI 10.1007/s40830-016-0097-5

SPECIAL ISSUE: NOVEL SHAPE MEMORY ALLOYS - BEHAVIOR AND PROCESSING, INVITED PAPER

# Shape-Memory Effect and Pseudoelasticity in Fe–Mn-Based Alloys

**P. La Roca[1,2] · A. Baruj[1,2] · M. Sade[1,2]**



**Abstract** Several Fe-based alloys are being considered as potential candidates for applications which require shape-memory behavior or superelastic properties. The possibility of using fabrication methods which are well known in the steel industry is very attractive and encourages a large amount of research in the field. In the present article, Fe–Mn-based alloys are mainly addressed. On the one hand, attention is paid to the shape-memory effect where the alloys contain (a) a maximum amount of Mn up to around 30 wt%, (b) several possible substitutional elements like Si, Cr, Ni, Co, and Nb and (c) some possible interstitial elements like C. On the other hand, superelastic alloys are analyzed, mainly the Fe–Mn–Al–Ni system discovered a few years ago. The most noticeable properties resulting from the martensitic transformations which are responsible for the mentioned properties, i.e., the fcc–hcp in the first case and the bcc–fcc in the latter are discussed. Selected potential applications are also analyzed.

**Keywords** Shape-memory effect · Superelasticity · Fe-based alloys · Steels · Fe–Mn-based alloys · Martensitic transformations

✉ M. Sade
sade@cab.cnea.gov.ar

[1] Centro Atómico Bariloche (CNEA) and Instituto Balseiro (U.N. Cuyo/CNEA), Av. E. Bustillo km 9, 5 (8400) S.C. de Bariloche, Río Negro, Argentina

[2] Consejo Nacional de Investigaciones Científicas y Técnicas (CONICET), Río Negro, Argentina

## Introduction

Fe-based shape-memory alloys constitute an attractive alternative to the most analyzed shape-memory materials, mainly Ni–Ti and Cu-based alloys [1–8]. The main reason is that the steel technology would be available for the fabrication of the alloys if proper applications were found. The main properties that characterize shape-memory materials are the one-way shape-memory effect, which is usually mentioned simply as shape-memory effect (SME), pseudoelasticity (also called superelasticity), and the two-way shape-memory effect (TWSME) [9]. The SME can be described as the recovery of the original shape by heating a material previously deformed. Superelasticity (SE) describes the shape recovery during unloading after deforming the material by stressing it [10, 11]. The TWSME is characterized by macroscopic shape changes related to temperature changes in both directions, heating and cooling. Reversible deformations can reach large values depending on the system; in some cases, they could be two orders of magnitude larger than the maximum elastic deformation [9]. Nowadays, there are many systems which exhibit one, two, or all the mentioned properties. These properties are due to martensitic transitions, i.e., non-diffusive solid–solid structural transformations which take place between the so-called austenite phase, and a second structure usually named martensite [12–14]. In Fe–Mn-based systems the austenite is retained by quenching from the high-temperature stable phase. In this way, the formation of non-transforming stable phases during cooling is avoided. The martensitic transition is usually thermally or mechanically induced and has been found in different metallic systems as well as in ceramics [15–18]. The presence of shape-memory effect and/or superelasticity will depend on the properties of the martensitic transformation taking place in the analyzed

Published online: 27 December 2016

system. Although a martensitic transformation is required for a system to become a shape-memory material, this condition is not sufficient to guarantee a shape-memory behavior. Also, there are materials which show superelasticity and SME, while others only display the SME [19]. The TWSME usually requires a specific thermomechanical treatment (so-called training treatment) to develop, although it has been shown in some cases that the training of the material might not be necessary if internal stresses are introduced [20–22]. It is clear then that understanding and improving shape-memory properties require a deep comprehension of martensitic transformations, the properties of the involved phases, and the relative phase stability between them. Martensitic transitions usually belong to the first-order type and are characterized by a hysteresis either if they are thermally or stress-induced. This hysteresis is one of the available characteristics for potential dissipative applications.

Using Fe-based shape-memory alloys could be more convenient than using other widely studied systems like Cu- and Ni–Ti-based alloys for a couple of additional reasons. Polycrystalline Cu-based shape-memory alloys are rather brittle and Ni–Ti, which has the noticeable advantage of being biocompatible, is comparatively expensive and might fracture for deformations higher than 30%. Fe-based alloys are not only attractive due to their lower cost but also due to their large deformability, good weldability, and good corrosion properties. This article focuses on Fe–Mn-based shape-memory alloys although some comments will be added concerning other systems when considered convenient. In particular, some selected topics will be analyzed here emphasizing the main characteristics of the martensitic transitions responsible for the shape-memory behavior. Selected systems will be discussed in greater detail.

Reported martensitic transformations in Fe-based systems are the fcc–fct, fcc–bcc or –bct, bcc–fcc, and fcc–hcp [23, 24]. These transitions are present in several systems. In some cases, a given system could show more than one martensitic transition depending on the composition and on the applied thermomechanical treatment. The fcc–hcp transition is responsible for the SME found in Fe–Mn-based alloys and the bcc–fcc is responsible for the superelastic effect reported in the Fe–Mn–Al–Ni system. These alloys and the corresponding martensitic transformations will be mainly addressed here although a few comments will be included concerning the fcc–bct transformation system. In the first place, the fcc–hcp transition will be analyzed as well as some significant findings in representative systems. The analysis of superelasticity mainly in the Fe–Mn–Al–Ni system will follow and finally selected potential applications will be discussed.

## The fcc–hcp Transition and the SME in the Fe–Mn System

The fcc–hcp transition has been extensively studied since the SME has been detected in Fe-based alloys. In particular, most of the research concerning the SME in these alloys has been performed in Fe–Mn-based alloys, with addition of Si, Cr, Co, and Ni. Several additional elements like Nb and C have also been considered as they will be commented below.

Main characteristics concerning the fcc–hcp transitions have been extensively studied in Fe–Mn binary alloys. The fcc austenite structure is stable at high temperatures and it is possible to have it in a metastable state at room temperature by quenching. In this alloy system, the martensite is hcp and it is metastable. Both phases are unordered substitutional solid solutions [25]. For Mn contents between 13 and 30 wt% approximately, the fcc–hcp martensitic transition takes place at temperatures close to the ambient one [26–28]. One of the main parameters which characterize the fcc–hcp transition is the volume change per atom, which is close to 2% [29]. There is no way to accommodate this volume change by an elastic deformation. An interesting consequence related to this relatively large volume change is that defects must be introduced in the material during transformation. Thus, at least one of the involved phases has to accommodate plastic deformation. This characteristic makes it extremely difficult or even impossible to thermally transform 100% of the material [30]. Therefore, attention must be paid to the definition of the martensitic transformation temperatures in this system. $M_s$ and $A_s$ are defined as usual as the temperatures to start the austenite to martensite transition and the reverse transition, respectively. Likewise, $A_f$ indicates the end of the retransformation, and it usually describes the temperature where the hcp–fcc transition is complete. However, in this system the so-called $M_f$ temperature is defined as the temperature where the transformation process ends, independently of the amount of formed martensite. Different mechanisms have been suggested to explain the martensitic transition [31–37]. However, the most accepted explanation considers that the hcp structure is formed by the overlapping of stacking faults and will be shortly commented here [32, 33]. The fcc structure can be described as a stacking of compact planes ($\{111\}_{fcc}$ type), usually named as ABCABC… If every two planes the lattice is shifted parallel to one of these planes in one of the $a/6\langle 112\rangle_{fcc}$ directions, stacking faults are created, leading to a local hcp stacking ABAB [38], as it is represented in Fig. 1. Several stacking faults spaced every two $\{111\}_{fcc}$ planes form an embryo of the hcp phase. These embryos can act as nucleation sites for the transition. Figure 2 shows

two TEM images of a Fe–Mn–Si-based alloy where austenite and martensite can be observed. In both cases, the zone axis is $[011]_{fcc}$. In Fig. 2a, martensite regions appear in the form of thin lines or thicker plates with a darker contrast. The traces of all these lines and plates are consistent with the direction of $\{111\}_{fcc}$ planes. A closer examination of martensite plates show that they are heavily faulted, as it can be seen in Fig. 2b. This feature is related to the mentioned transformation mechanism. As the material could miss the sequence of one stacking fault every two at some point, a defect in the stacking sequence is inherited by the martensite.

Dislocations with $a/6\langle 112\rangle_{fcc}$ Burgers vector are usually known as partial or Shockley dislocations and can be introduced by the splitting of perfect dislocations. An interesting point arises if displacements in the three possible Burgers vectors belonging to a specific $(111)_{fcc}$ plane take place in an aleatory way. In this case, three variants will form in the same plane, while the total shape change will be compensated by each one and no significant macroscopic shape change will be evident. This is what usually happens during thermally induced fcc–hcp transitions [39]. However, if the transition is mechanically induced, a particular Burgers vector might be favored according to the applied stress mode, leading to a measurable shape change [40]. Although this is a requirement for the existence of the shape-memory effect, it is not enough to obtain a complete recovery, as it has been noticed for Fe–Mn alloys where partial shape recovery was reported [41, 42]. An additional needed condition is to retransform from hcp to fcc by reversing the path the material used for the direct transformation, i.e., the retransformation should take place by the coalescence of the same partial dislocations which formed during the fcc–hcp transition [43]. An incomplete SME can be explained by different factors: a retransformation taking place by shears different from those operative during the fcc–hcp transition and the interaction between partial dislocations with different obstacles like defects, α' plates, or other hcp plates [44, 45].

Another significant point to consider in the Fe–Mn system is the magnetic transition of the austenite. The fcc structure shows a para- to antiferromagnetic transition at the so-called Néel temperature ($T_N^{fcc}$) which increases with the increment of Mn content. An increase in Mn amount also produces a decrease in $M_s$ which varies approximately linearly with Mn content in the composition range where $T_0 > T_N^{fcc}$, being $T_0$ the temperature where Gibbs energies for austenite ($G^{fcc}$) and martensite ($G^{hcp}$) are the same [27]. This is the case for Mn content up to 25 wt% approximately. The effect of the magnetic transition on the martensitic one can be understood if the Gibbs energies are considered for both phases. Usually, not far from $T_0$, it is accepted that Gibbs energies might decrease linearly with a temperature increase, the amount of this decrease is directly related with the entropy of the structure. Decreasing the temperature below $T_0$, a required driving force for the fcc–hcp transition implies the need of an undercooling down to $M_s$. It has been shown that the magnetic ordering of the fcc structure alters the change of $G^{fcc}$ with temperature, producing an stabilization of this phase. Further cooling is then required to reach the necessary driving force for the transformation. This explains the strong decrease of $M_s$ observed in Fe–Mn alloys and also in higher-order systems once the fcc structure becomes magnetically ordered, which might even lead to the complete inhibition of the martensitic transformation [27]. For Mn contents smaller than 16% approximately, a bcc martensite (α') is formed, which is also a metastable structure in this case with a ferromagnetic order [46]. This martensite coexists in some cases with the hcp martensite and might affect the SME. The

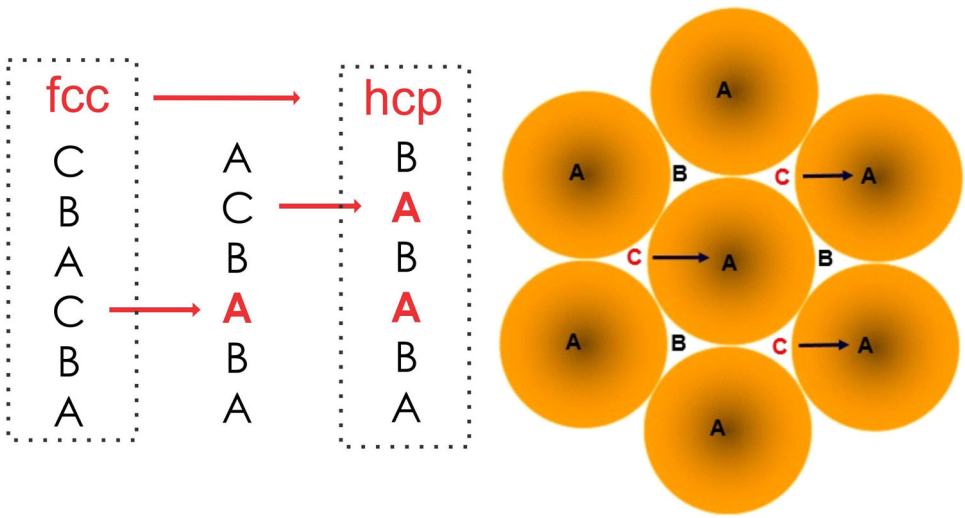


**Fig. 1** Schematic representation of the fcc–hcp martensitic transformation mechanism

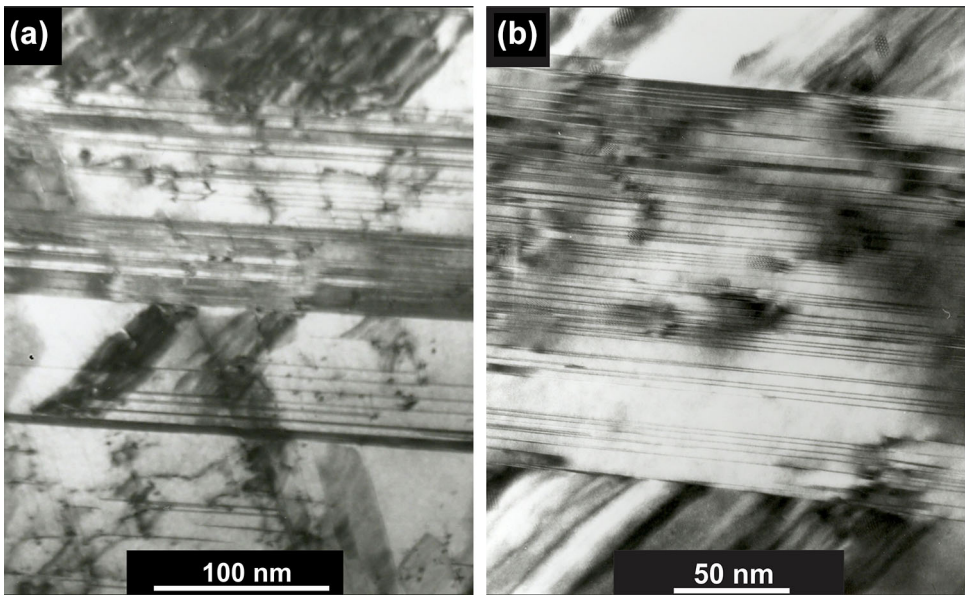


**Fig. 2** TEM images of austenite and martensite in a Fe–Mn–Si-based alloy. The zone axis is $[011]_{fcc}$. **a** Martensite appears in the form of *lines* or plates with a *darker contrast*. **b** Detail of a martensite plate. The plate contains several stacking faults, which appear as *parallel lines* inside it

addition of other elements to the Fe–Mn binary system might affect the magnetic transition of the austenite, the volume change between austenite and martensite, and the stacking fault energy; all these properties being relevant to understand the effect of alloying on the shape-memory behavior. An additional aspect should also be taken into consideration here: once it is accepted that the deformation accompanying the fcc–hcp transition cannot be elastic due to the volume change, it is understandable that mechanical properties of each structure play a significant role in the material behavior. As an example, the fcc austenite is usually easier to deform in comparison with the hcp martensite.

## On the fcc–hcp Martensitic Transition in Fe–Mn-Based Alloys

The Fe–Mn–Si system deserves particular attention mainly due to the following reasons. On one hand, it was the first Fe–Mn-based system where a large SME was detected. This was found in single crystals of Fe–Mn–Si alloys and later in polycrystalline alloys too. On the other hand, most of the higher-order alloys with additional components (Cr, Co, C, Ni) reported as candidates for getting a good shape-memory behavior do keep Si as a significant component. A nearly complete SME in Fe–Mn–Si single crystals was first reported in 1982 by Sato et al. [47]. Later on, good results were obtained in polycrystalline Fe–Mn–Si alloys subjected to training treatments [48, 49]. Amounts of Si between 5.0 and 6.5 (wt%) are considered a good choice for optimum SME. The main reasons that explain the positive contribution of Si can be found on the effect this element has on the Néel temperature of the austenite and on the stacking fault energy [50, 51]. Both magnitudes decrease if Si is added. The decrease in the Néel temperature enhances the fcc–hcp transition by increasing the available driving force while the effect on the stacking fault energy facilitates nucleation of the martensite. A strengthening effect has been reported, which enhances the reversibility of the transition, and a decrease in the volume change with addition of Si to the Fe–Mn system, reported by Nikolin et al., might also favor a larger reversibility in the fcc–hcp transformation [51, 52]. The effect of Si on the martensitic transformation temperature deserves some attention. Values of the critical transformation temperatures have been reported by several authors, leading to some scatter if defined dependences on composition are desired [53]. An experimental analysis of a large amount of alloys in the range 16–33 wt% of Mn, containing up to 6 wt% Si, indicated that $M_s$ increases for constant Mn content up to 4 wt% Si approximately, showing a slight opposite tendency for larger amounts of Si (Fig. 3) [54]. A thermodynamic analysis where the Gibbs energies of fcc and hcp structures were calculated leads to the estimation of the driving forces which operate at $M_s$. Considering constant Si lines, the driving forces increase with Mn content increase. In turn, considering constant Mn, the driving forces at the transformation decrease if Si is added [55]. These results reinforce the idea that Si addition has a positive effect on the fcc–hcp transition. It should, however, be kept in mind that critical transformation temperatures do depend on the microstructure. As an example, the introduction of defects by thermal cycling of Fe–Mn–Si alloys through the fcc–hcp transformation slightly decreases $M_s$ while $A_s$ increases [56, 57]. In fact, the introduction of defects by thermal cycling leads to changes in critical temperatures in several analyzed Fe–Mn-based systems. Particularly, in the binary system, a promotion effect in the

first cycles and an inhibition of the direct transformation after further cycling has been reported; a phenomenon also reported in the Fe–Mn–Co system [58, 59]. This rather contradictory effect was explained by the introduction of stacking faults at initial stages of production of defects while perfect dislocations are introduced after further cycling or larger deformation amounts.

Another important parameter to consider is grain size because it affects transformation temperatures and the degree of shape recovery. For example, the $M_s$ temperature of Fe–Mn alloys strongly decreases when grain size becomes smaller than 30 μm, while the shape recovery in Fe–Mn–Si alloys is increased for grain sizes smaller than 60 μm [60, 61]. An interesting fact to consider is the need of training of the Fe–Mn–Si system in order to introduce a reasonable amount of shape recovery and a large recovery stress [62]. This training might be introduced by different thermomechanical methods, which mainly include deforming and heating above a selected temperature, several repetitions usually being required. Training was considered as an additional method to strengthen the austenite and a convenient way to introduce a high amount of stacking faults. The need of improving the corrosion resistance and the requirement of finding more convenient industrial procedures lead to the addition of other elements and/or looking for alternative methods to avoid training.

The addition of Cr or Cr and Ni to the Fe–Mn–Si system has been considered to reduce corrosion [63–65]. Different approaches can be used to analyze the effect of adding these elements. On one hand, tests that measure shape-memory recovery and recovery stress are specifically required to determine if the contribution is significant for the improvement of shape-memory properties. On the other hand, each one of the mentioned elements might affect in a different way the relative phase stability between austenite and martensite, which involves driving forces, martensitic transformation temperatures, lattice parameters, magnetic ordering, stacking fault energy, strength of the phases, etc. A comprehensive analysis would require knowing all these effects which, for the time being, are only partially understood. The effect of Cr on the corrosion resistance is well known, and is related to the formation of a surface layer which protects the bulk material [66]. However, Cr addition also affects the martensitic transformation temperatures and $T_N^{fcc}$ [63, 67]. Both effects are to be considered to design new alloys. The addition of Cr to the Fe–Mn system leads to a decrease in $M_s$ and in $T_N^{fcc}$. The variation of $M_s$ with Cr is linear at constant Mn and becomes clearly stronger if $M_s$ becomes smaller than $T_N^{fcc}$. Cr contents higher than 7 wt% lead to the formation of the sigma phase, increasing brittleness. This problem can be neutralized by the addition of Ni.

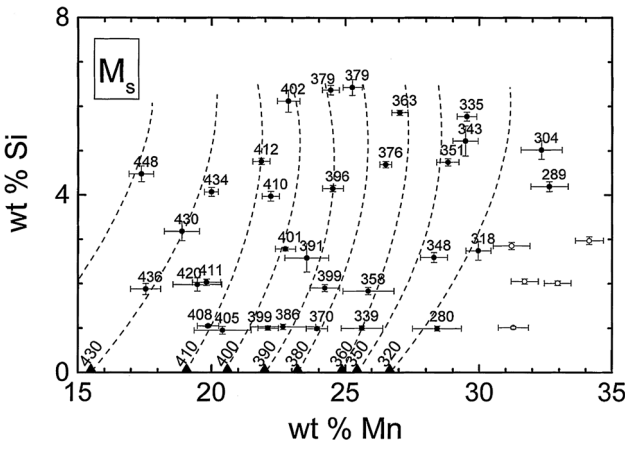


**Fig. 3** $M_s$ temperatures corresponding to the fcc–hcp martensitic transformation for different Fe–Mn–Si alloys [54]. Temperature values are expressed in K. Reprinted from Ref. [54], Copyright (1998), with permission from Elsevier

The positive effect of training on the improvement of the SME is also observed in the Fe–Mn–Si–Cr and Fe–Mn–Si–Cr–Ni systems, and including also Co or other elements as it was reported by many authors [68]. In all cases, a strong increase in the shape recovery and in the recovery stress was found. For each case, the amount of deformation, time, and temperature of aging must be optimized. Additionally, the free recovery before the recovery stress becomes operative must be analyzed specifically for each alloy and selected training method. Several microstructural analyses of Fe–Mn–Si alloys allowed to understand the main effects of training on the material which can be summarized as follows: hcp plates become thinner; their distribution becomes more homogeneous; the number of hcp variants decreases; and a large amount of stacking faults are created [69, 70]. Finally the matrix becomes harder due to the introduction of plastic deformation.

It is understandable that once the consequences of training became known, research would focus on getting the same advantages with alternative methods, with higher possibilities to be included in industrial procedures. Main attempts looked for the strengthening of the matrix by introducing plastic deformation, addition of other elements or introduction of precipitates [71–74]. The main desired output would be the decrease of irreversibility during the martensitic transformation. Thermomechanical treatments have been suggested in this direction in the composition range ($15 < \text{wt\% Mn} < 32$, $1 < \text{wt\% Si} < 6$) [75, 76]. An interesting example of this research included the addition of small amounts of Nb and C leading to the precipitation of NbC, which followed a deformation by rolling. In fact it was shown that rolling and subsequently introducing NbC precipitates allowed to increase shape recovery up to approximately 100% for deformations close to 4%, with a strong increase in the recovery stress [77]. The main

conclusion of this is that training can be substituted by methods usually available in the steel industry, leading to a good shape recovery and large recovery stress. The main microstructural consequences of this thermomechanical procedure can be summarized as follows:

(a) Stacking faults are produced during the rolling step.
(b) The matrix is strengthened by part of the introduced plastic deformation which does not disappear after precipitation.
(c) Precipitates associate to stacking faults, favoring the homogeneous distribution of stacking faults, enhancing nucleation of selected hcp variants.
(d) Internal stresses due to the precipitates favor the retransformation to the original orientation of the austenite.
(e) Thin martensite plates are homogeneously distributed.

The mentioned effects on the microstructure clearly indicate that the comprehension of shape-memory behavior in Fe–Mn-based alloys has shown noticeable progress in the last years, becoming more attractive for applications. In fact, it has been recently reported that a large recovery strain can be reached by an adequate selection of microstructure [78].

## Superelasticity in Fe-Based Alloys

Recently, new superelastic Fe-based metallic systems have been developed based on Fe–Ni–Co and Fe–Mn–Al–Ni alloys [79, 80]. These findings have encouraged new research and brought large interest into the field. The main characteristics of the first alternative will be summarized, and more detailed analysis on the second system will be presented.

### The fcc–bct Martensitic Transformation in Fe–Ni–Co-Based Alloys

The martensitic transformation related to the superelastic properties is the fcc–bct. It has been shown that precipitates of an ordered structure $L1_2$ ($\gamma'$) form after aging. This precipitation changes the non-thermoelastic character of the transition to a thermoelastic one [79, 81]. Precipitates harden the austenite, decreasing irreversible plastic deformation, leading to a strong decrease in the thermal hysteresis [82, 83]. Excellent superelastic properties were reported in FeNiCoAlTa showing the fcc–bct martensitic transition, where reversible deformations as high as 13% are obtained in tensile mode [79]. This result was obtained in polycrystalline samples with $\gamma$ nanoprecipitates with an adequate control of grain size and texture. Further research addressed the attention on the effects of nanoprecipitates both in monocrystalline and polycrystalline FeNiCoAl-based alloys [84–94]. Very recently, the superelastic response of the $Fe_{41}Ni_{28}Co_{17}Al_{11.5}Nb_{2.5}$ (at.%) single crystals oriented along the [001] direction was investigated in tension and abnormally large reversible strain of up to 15.3% was observed at 77 K, the highest ever reported for an Fe-based shape-memory alloy [95].

### The bcc–fcc Martensitic Transformation in Fe–Mn–Al–Ni Alloys

#### *On the bcc–fcc Martensitic Transition*

The ternary $Fe_{49}Mn_{36}Al_{15}$ (at.%) alloy shows an unusual martensitic transformation from a high-temperature bcc austenite ($\alpha$) to a fcc martensite ($\gamma'$). This transition takes place at room temperature and is non-thermoelastic [24]. In ternary Fe–Mn–Al, the bcc ferritic phase ($\alpha$) becomes ferromagnetic at the Curie temperature $T_C^{\alpha}$. This transition stabilizes the $\alpha$ phase giving place to the known $\gamma$ loops in the phase diagram. Additionally, Al favors the stability of the $\alpha$ phase. If Mn is added up to 30%, the fcc $\gamma$ phase transforms to the martensitic $\alpha$', usual in ferrous alloys. However, after further increasing Mn content and for amounts of Al higher than 15 at.%, $T_C^{\alpha}$ decreases down around room temperature. In this way, the $\gamma$ loop is reduced, and a $\alpha \rightarrow \gamma'$ martensitic transition takes place at low temperatures, an extremely significant result [24, 80]. The martensitic transition takes place at temperatures lower than $T_C^{\alpha}$ which implies that the austenite is ferromagnetic while the martensite is weakly magnetic, due to the para- to antiferromagnetic transition occurring in the fcc structure at a Néel temperature close to 40°C [80]. The phase diagram of the Fe–Mn–Al system was experimentally studied as well as calculated using thermodynamic models [96]. In this way, it was possible to evaluate the composition and temperature range where the $\alpha$ phase forms and the influence of the magnetic interaction on the relationship between temperature and phase stability.

The thermoelastic character is obtained after the addition of Ni and precipitation of an ordered bcc structure (B2). Martensite variants grow during cooling and move back during heating in the quaternary $Fe_{43.5}Mn_{34}Al_{15}Ni_{7.5}$ (at.%) alloy after the introduction of Ni-rich nanoprecipitates [80]. Under this condition, the alloy becomes superelastic and large reversible deformations are attainable with two remarkable additional properties: (a) the effect of temperature on the critical transformation stress is weak if compared with other shape-memory alloys (Fig. 4), extending the temperature range for applications of this alloy, and (b) a strong magnetic change takes place simultaneously with the martensitic transformation. Both properties could lead to several applications as it will be commented below.

*Effects of the Microstructure*

Microstructure plays a significant role in the optimization of shape-memory properties in all the systems which show these particular behaviors. Just to mention some examples, reversibility is strongly enhanced in polycrystalline Cu-based alloys if the grain size is largely increased if compared with the sample size [97, 98]. Particularly, the so-called bamboo microstructure was found to be convenient for getting good superelastic and shape-memory properties in these alloys [98, 99]. Additionally, it has been reported that grain size affects the relative stability between involved phases in martensitic transitions, mainly increasing the stability of austenite when the grain size sufficiently decreases. This leads to a decrease of martensitic transformation temperatures and increase in hysteresis for small grains [99–101].

In the Fe–Mn–Al–Ni system, it has also been shown that the bamboo microstructure strongly favors superelasticity, which shows the significant role grain size plays in the enhancement of desired properties [80, 102, 103].

The introduction of precipitates adds another microstructural contribution which cannot be overlooked. This has also been shown in different metallic systems. A recent example has been reported in Cu–Zn–Al single crystals where the introduction of nanoprecipitates hardens the 6R martensite, enabling to have reversible superelastic deformation of 20% if two consecutive martensitic transformations are used (austenite-18R-6R) [104]. The effect of precipitates in Fe–Mn-based alloys concerning the fcc–hcp transition [105] and the role played by coherent precipitates in the thermoelastic properties of Fe–Ni–Co-based alloys have already been mentioned. Particularly, in Fe–Mn–Ni–Al alloys, the presence of coherent nanoprecipitates is also required to have thermoelastiticity and superelasticity [80, 106, 107]. It also seems that due to these precipitates, the martensite is distorted by the introduction of thin nanotwins [106].

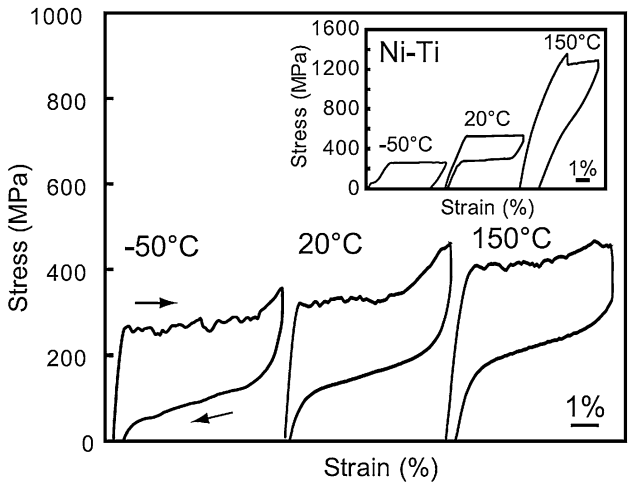


**Fig. 4** Pseudoelastic response of a Fe–Mn–Al–Ni alloy compared with NiTi [80]. From Ref. [80]. Reprinted with permission from AAAS

It has been reported that after compressing a single-crystalline sample of $Fe_{43.5}Mn_{34}Al_{15}Ni_{7.5}$ in direction $\langle 001 \rangle$, larger reversibility is obtained if compared with a similar experiment performed under tensile load and same orientation where only one variant was induced [107]. The same authors analyzed the evolution of precipitation during aging at 200°C showing that after 3 h at this temperature the obtained distribution and size of B2 precipitates lead to the largest superelastic reversibility [108]. A still larger reversible deformation (7.8%) was found for tensile stress-induced martensite of austenitic single crystals oriented parallel to $\langle 123 \rangle_{\alpha}$. This was explained by the introduction of two variants which should make it easier to accommodate the required deformation decreasing the introduction of dislocations [109].

Addressing the research to polycrystalline material, Vollmer et al. reported the introduction of cracks in grain boundaries of the $\alpha$ phase after the rapid quench in water of $Fe_{43.5}Mn_{34}Al_{15}Ni_{7.5}$ samples [110]. By decreasing the cooling speed from the solution treatment, the formation of cracks is inhibited thanks to the formation of the ductile $\gamma$ phase at grain boundaries; however, this might have a detrimental effect on reversibility [110]. The effect of cycling on samples showing the bamboo microstructure was also analyzed indicating that a degradation of the superelastic effect takes place due to the introduction of dislocations, being also dependent on the orientation of each grain [111]. The change of the microstructure by selective laser melting was also explored getting textures of columnar microstructures with a promising pseudoelastic performance [112].

A final comment to this point concerns the method to obtain the bamboo microstructure which leads to a large reversible deformation. Omori et al. have shown that thermal cycling between 1200 °C ($\alpha$ phase region) and 600 to 1000 °C ($\alpha + \gamma$ phase region) produces an abnormal grain growth leading to a grain size close to 30 mm after 10 cycles [113].

## On Potential Applications

There is no doubt that the properties exhibited by shape-memory alloys are noticeably different from those present in most of the materials and this difference is a permanently attractive challenge for the development of applications. The main properties which are considered for the applications are superelasticity and SME [23, 114]. Both properties mainly exhibit the ability of recovering large deformations by the use of martensitic transformations.

There are several metallic systems showing these properties but interest is mainly focused on those which enable deformation recoveries larger than 4% or enable the application of large forces during a constrained recovery [114].

One of the pioneer applications is the use of coupling for different types of tubes. The first used metallic system for this was the NiTi alloy developed by Raychem in the 70′s to be used for couplings of Ti tubes in F14 airplanes avoiding in this way the complicated welding process [114]. Couplings of NiTiFe were obtained by machining rings down to an internal diameter smaller than the external one of the tubes to be joined. These rings were stress expanded at low temperatures, and not being able to recover their shape after bringing them to work temperature they apply a force on the tubes. The property which is used in this case is the recovery stress associated to the martensite–austenite transformation present in the SME. Two drawbacks complicate the use of NiTi couplings for a large amount of different applications: cost of the alloy and the need of expanding and keeping the couplings at low temperatures till the moment of using them.

Alternative metallic systems like Cu-based and Fe–Mn–Si-based alloys have been studied to find a solution for the mentioned problems [8, 23, 114, 115]. Both alternatives would strongly decrease cost if compared with NiTi alloys and, additionally, are easy to machine and weld. However, Cu-based alloys show low ductility and change their properties due to stabilization of the martensite at temperatures not far from room temperature. On the other hand, Fe–Mn–Si improves their properties by a training process which increases reversibility and shape recovery stress, this training is a strong complication for industrial manufacturing. Anyway, research on the best training methods has been the target of a large amount of work and is still a challenge [70, 116].

Fe–Mn-based shape-memory alloys are considered as a interesting alternative to be used for pipe couplings [115, 117–119] and to reinforce concrete [120]. The first possibility is based on the same concepts used with the first couplings of NiTi, i.e., the shape recovery stress is the main property to be used here, which should remain stable during long time periods. In the reinforcement of concrete, coils are to be used or even other material shape might be possible. The SMA should be deformed and included in the plaster matrix. Once the matrix becomes solid, the SMA should be heated leading to a constrained recovery and the generation of internal compressive stresses in the concrete.

In both cases, it is still rather difficult to evaluate the internal stresses that originated in the constrained recovery and their variations due to changes in temperature or applied stresses.

Concerning the applications of superelasticity, among the most promising ones, the use of SMA in the systems to be used for damping in seismic events is considered. Fe–Mn–Al–Ni might be a good alternative here, mainly due to the large hysteresis and light change of critical transforming stress with temperature.

Other interesting applications to be considered are those which use the strong change in magnetization of these alloys. It has been shown that during stress-induced transformations of melt spun ribbons of $Fe_{43.5}Mn_{34}Al_{15}Ni_{7.5}$, large variations in the magnetic permeability are detected ($\approx 12\%$), even for small reversible deformations ($\approx 0.5\%$) [121]. Sensing deformations with no contact is a promising application.

Interesting additional applications might use the mechanical properties related with the stress-induced fcc–hcp transition, exhibited by Fe–Mn-based alloys. Particularly, high-manganese steels have been considered as an attractive system due to the plasticity associated with martensitic transformations. Positive performance related with high ductility, high strength and mechanical resistance, deformation hardening and strong elasto-plastic damping have been reported for Fe–Mn–Si-based alloys [122–125]. These properties might lead to the development of damping systems to decrease the damage in building during natural seismic events [126–128].

Although some applications have been commented in this article, a detailed analysis of possible applications including cost analysis has been recently published [129]. Finally, the transformation from many of these ideas into useful industrial applications is still a strong challenge for the near future.

**Acknowledgements** The authors thank ANPCyT Argentina (PICT 2012-0884), CONICET (PIP 0513 and PIP 0056), and U.N. Cuyo (06/C516) for their financial support.

## References

1. Sohmura T, Oshima R, Fujita FE (1980) Thermoelastic fcc-fct martensitic transformation in Fe-Pd alloy. Scripta Metall. 14(8):855–956
2. Kajiwara S (1985) Nearly perfect shape memory effect in Fe-Ni-C alloys. Trans JIM 26(8):595–596
3. Oshima R, Sugimoto S, Sugiyama M, Hamada T, Fujita FE (1985) Shape memory effect in an ordered Fe//3Pt alloy associated with the fcc-fct thermoelastic martensite transformation. Trans Jpn Inst Metals 26:523–524
4. Murakami M, Suzuki H, Nakamura Y (1987) Effect of Si on the shape memory effect on polycrystalline Fe-Mn-Si alloys. Trans ISIJ 27:87
5. Maki T, Furutani S, Tamura I (1989) Shape memory effect related to thin plate martensite with large thermal hysteresis in ausaged Fe-Ni-Co-Ti alloy. ISIJ Int 29(5):438–445

6. Koval YuN, Monastyrsky GE (1993) Reversible martensite transformation and shape memory effect in Fe-Ni-Nb alloys. Scr Metall 28(1):41–46
7. Maki T (1998) Martensitic transformations: crystallography. In: Otsuka K, Wayman CM (eds) Shape memory materials. Cambridge University Press, Cambridge
8. Kajiwara S (1999) Characteristic features of shape memory effect and related transformation behavior in Fe-based alloys. Mater Sci Eng A 273–275:67–68
9. Otsuka K, Wayman CM (1998) Mechanism of shape memory effect and superelasticity. In: Otsuka K, Wayman CM (eds) Shape memory materials (Chapter 2). Cambridge University Press, Cambridge, pp 27–48
10. Krishnan RV, Delaey L, Tas H, Warlimont H (1974) Thermoplasticity, pseudoelasticity and the memory effects associated with martensitic transformations - Part 2 The macroscopic mechanical behavior. J Mater Sci 9(9):1536–1544
11. Wollants P, Roos JR, Delaey L (1993) Thermally-and stress-induced thermoelastic martensitic transformations in the reference frame of equilibrium thermodynamics. Prog Mater Sci 37(3):227–288
12. Cohen M, Olson GB, Clapp PC (1979) On the classification of displacive phase transformation. In: Proceedings of the international conference on martensitic transformations, Ed. By Department of Materials Science and Engineering, MIT, Cambridge vol 02139, pp 1–11
13. Christian JW, Olson GB, Cohen M (1995) Classification of displacive transformations: What is a martensitic transformation? J Phys IV C8 V5:3–10
14. Roytburd AL (1999) Kurdjumov and his school in martensite of the 20th century. Mater Sci Eng A 273–275:1–10
15. Saburi T (1998) Ti-Ni shape memory alloys. In: Otsuka K, Wayman CM (eds) Shape memory materials, Chapter 3. Cambridge University Press, Cambridge, pp 49–96
16. Ahlers M (1986) Martensite and equilibrium phases in CuZn and CuZnAl alloys. Prog Mater Sci 30(3):135–186
17. Simha NK (1995) Crystallography of the tetragonal → monoclinic transformation in Zirconia. J Phys IV 5(C8): 1121–1126
18. Hayakawa M, Okuda T, Oka M (1995) Grain size dependence of the martensitic transformation of Yttria doped tetragonal zirconia polycrystals. J Phys IV 5(C8):1127–1132
19. Otsuka K, Wayman CM, Nakai K, Sakamoto H, Shimizu K (1976) Superelasticity effects and stress-induced martensitic transformations in Cu-Al-Ni alloys. Acta Metall 24:207–226
20. Eucken S, Duerig TW (1989) The effects of pseudoelastic prestraining on the tensile behaviour and two-way shape memory effect in aged NiTi. Acta Metall 37(8):2245–2252
21. Pons J, Sade M, Lovey FC, Cesari E (1993) Pseudoelastic cycling and two-way shape memory effect in β Cu-Zn-Al alloys with γ-precipitates. Mater Trans JIM 34:888–894
22. Isalgué A, Lovey FC, Sade M, Torra V (1995) Anisotropic behavior in Cu-Zn-Al SMA due to the oriented growth of gamma precipitates. J Phys Colloq 5(C2):153–158
23. Otsuka K, Wayman CM (1998) Shape memory materials. Cambridge University Press, Cambridge
24. Ando K, Omori T, Ohnuma I, Kainuma R, Ishida K (2009) Ferromagnetic to weak-magnetic transition accompanied by bcc to fcc transformation in Fe-Mn-Al alloy. Appl Phys Lett 95(21):212504
25. Huang W (1989) An assessment of the Fe-Mn system. CALPHAD 13(3):243–252
26. Troiano AR, McGuire FT (1943) A Study of the Iron-Rich Iron-Manganese Alloys. Trans Am Soc Metals 31:340–364
27. Cotes SM, Sade M, Guillermet AF (1995) Fcc/Hcp martensitic transformation in the Fe-Mn system: Experimental study and thermodynamic analysis of phase stability. Metall Mater Trans A 26(8):1957–1969
28. Cotes SM, Baruj A, Sade M, Guillermet AF (1995) Thermodynamics of the γ/ε martensitic transformation in Fe-Mn alloys: modelling of the driving force, and calculation of the Ms and As temperatures. J. Phys IV 5(C2):83–88
29. Marinelli P, Sade M, Guillermet AF (2002) On the structural changes accompanying the fcc/hcp martensitic transformation in Fe-Mn-Co alloys. Scr Mater 46:805–810
30. Schumann H, Heider F (1965) Einfluss wiederholter Phasenubergange auf die γ-ε-Umwandlung in austenitischen Manganstahlen. Z Metallkd 56:165–172
31. Bollman W (1961) On the phase transformation of cobalt. Acta Metall 9:972–975
32. Fujita H, Ueda S (1972) Stacking faults and f.c.c. (γ) → h.c.p. (ε) transformation in 188-type stainless steel. Acta Metall 20:759–767
33. Cotes SM, Guillermet AF, Sade M (2004) Fcc/Hcp martensitic transformation in the Fe-Mn system: part II. Driving force and thermodynamics of the nucleation process. Metall Mater Trans A 35A:83–91
34. Horsewell A, Ralph B, Howell PR (1975) Intergranular mechanism for the f.c.c. yields h.c.p. martensitic transformation. Phys Status Solidi 29(2):587–594
35. Sato A, Sunaga H, Mori T (1979) Reversibility of γ → ε transformation in Fe-18Cr-Ni alloy single crystals. In: Proceedings of ICOMAT, Cambridge, American Institute of Metals, pp 183–188
36. Inagak H (1992) Shape memory effect of Fe-14%Mn-6%Si-9%Cr-6%Ni alloy polycrystals. Zeitschrift für Metallkunde 83:90–96
37. Hsu TY, Zuyao X (1999) Martensitic transformation in Fe-Mn-Si based alloys. Mater Sci Eng A 273–275:494–497
38. Olson GB, Cohen M (1976) A general mechanism of martensitic nucleation: Part I. General concepts and the FCC → HCP transformation. Metall Trans A 7(12):1897–1904
39. Putaux J-L, Chevalier J-P (1996) HREM study of self-accommodated thermal ε-martensite in an Fe-Mn-Si-Cr-Ni shape memory alloy. Acta Mater 44(4):1701–1716
40. Bergeon N, Guenin G, Esnouf C (1997) Characterization of the stress-induced e martensite in a Fe-Mn-Si-Cr-Ni shape memory alloy: Microstructural observation at different scales, mechanism of formation and growth. Mater Sci Eng A 238(2):309–316
41. Enami K, Nagasawa A, Nenno S (1975) Reversible shape memory effect in Fe-base alloys. Scr Metall 9(9):941–948
42. Tsuzaki K, Ikegami M, Tomota Y, Maki T (1990) Effect of transformation cycling on the ε martensitic transformation in Fe-Mn alloys. ISIJ Int 30:666–673
43. Jian L, Wayman CM (1992) On the mechanism of the shape memory effect associated with γ(fcc) to ε(hcp) martensitic transformations in Fe-Mn-Si based alloys. Scr Metall Mater 27(3):279–284
44. Baruj A, Cotes S, Sade M, Guillermet AF (1996) Effects of thermal cycling on the Fcc/Hcp martensitic transformation temperatures in the Fe-Mn system: Thermodynamic analysis, systematic aspects and microstructural interpretation. Zeit fuer Metallkde 87(10):765–772
45. Baruj A, Troiani HE, Sade M, Guillermet AF (2000) Effects of thermal cycling on the fcc/hcp martensitic transformation temperatures in the Fe-Mn system: Part II. TEM study of the microstructural changes. Philos Mag A 80:2537–2548
46. Nishiyama Z (1978) In: Cohen M, Meshii M, Wayman CM (eds) Martensitic transformations. Academic Press, New York
47. Sato A, Soma K, Chishima E, Mori T (1982) Shape memory effect and mechanical behavior of an Fe-30Mn-1Si alloy single crystal. J Phys 43(C4):797–802

48. Murakami M, Otsuka H, Suzuki H, Matsuda S (1986) Effect of alloying content, phase and magnetic transformation on the shape memory effect of Fe-Mn-Si alloys. Trans ISIJ 27:B-88
49. Murakami M, Otsuka H, Suzuki H, Matsuda S (1986) Improvement in shape memory effect for Fe-Mn-Si alloys. Trans ISIJ 27:B-89
50. Hsu TY, Zuyao X (1999) Martensitic transformation in Fe-Mn-Si based alloys. Mater Sci Eng A 273–275:494–497
51. Murakami M, Otsuka H, Suzuki HG, Matsuda S (1986) Complete shape memory effect in polycrystalline Fe-Mn-Si alloys. In: Proceedings of The international conference in martensitic transformation (ICOMAT-86), The japan institute of metals, pp 985-990
52. Nikolin BI, Sokolov OG, Lysak LI, Makogon YuN (1977) Influence of silicon and manganese in the lattice parameter of $\gamma$ and $\varepsilon$ phases and volume effects of the $\gamma \rightarrow \varepsilon$ transformation in alloys of the G20 type. Phys Met Metall 44(3):639–642
53. Baruj A, Cotes S, Sade M, Guillermet AF (1995) Coupling binary and ternary information in assessing the fcc/hcp relative phase stability and martensitic transformation in Fe-Mn-Co and Fe-Mn-Si alloys. J Phys Colloq 5(C8):373–378
54. Cotes S, Guillermet AF, Sade M (1998) Phase stability and fcc/hcp martensitic transformation in Fe-Mn-Si alloys. Part I. Experimental study and systematics of the Ms and As temperatures. J Alloys Comp 278:231–238
55. Cotes S, Guillermet AF, Sade M (1998) Phase Stability and fcc/hcp martensitic transformation in Fe-Mn-Si alloys: Part II. Thermodynamic modelling of the driving forces and the Ms and As temperatures. J. Alloys Comp 280:168–177
56. Sade M, Halter K, Hornbogen E (1988) The effect of thermal cycling on the transformation behavior of Fe-Mn-Si Shape memory alloys. Z fuer Metallkunde 79(8):487–491
57. Andrade MS, Osthues RM, Arruda GJ (1999) The influence of thermal cycling on the transition temperatures of a Fe-Mn-Si shape memory alloy. Mater Sci Eng A 273–275:512–516
58. Baruj A, Cotes S, Sade M, Guillermet AF (1996) Effects of thermal cycling on the Fcc/Hcp martensitic transformation temperatures in the Fe-Mn system: Thermodynamic analysis, systematic aspects and microstructural interpretation. Zeit fuer Metallkde 87(10):765–772
59. Baruj A, Guillermet AF, Sade M (1999) Effects of thermal cycling and plastic deformation upon the Gibbs energy barriers to martensitic transformation in Fe-Mn and Fe-Mn-Co alloys. Mater Sci Eng A 273–275:507–511
60. Takaki S, Nakatsu H, Tokunaga Y (1993) Effects of austenite grain size on $\varepsilon$ martensitic transformation in Fe-15mass% Mn Alloy. Mater Trans JIM 34:489–495
61. Shiming T, Jinhai L, Shiwei Y (1991) Two-way shape memory effect of an Fe-Mn-Si alloy. Scr Metall Mater 25:2613–2615
62. Li H, Dunne D, Kennon N (1999) Factors influencing shape memory effect and phase transformation behavior of Fe-Mn-Si based shape memory alloys. Mater Sci Eng A 273–275:517–523
63. Troiani HE, Sade M, Bertolino G, Baruj A (2009) Martensitic transformation temperatures and microstructural features of FeMnCr Alloys. ESOMAT 2009:06002
64. Mertinger V, Benke M, Nagy E, Pataki T (2014) Reversible characteristics and cycling effects of the $\varepsilon \leftrightarrow \gamma$ martensitic transformations in Fe-Mn-Cr Twip/Trip steels. J Mater Eng Perform 23(7):2347–2350
65. Mertinger V, Benke M, Nagy E (2015) Effect of Cr Content on the TWIP Behavior in Fe-Mn-Cr Steels. Mater Today 2:S673–S676
66. Nishimura T (2014) Structure of the passive film formed on Fe-Mn-Si-Cr-Ni shape memory alloy after wet and Dry corrosion test. Mater Trans 55(6):871–876
67. Sade M, Baruj A, Troiani HE (2008) Fcc/hcp martensitic transformation temperatures and thermal cycling evolution in Fe-Mn-Cr alloys, New Developments on Metallurgy and Applications of High Strength Steels. In: Proceedings of the international conference new developments on metallurgy and applications of high strength steels, v2 physical metallurgy and alloy design, pp 1183–1191
68. Shiming T, Shiwey Y (1992) Effect of pre-strain on shape memory behavior of an Fe-Mn-Si-Cr-Ni-Co. Scr Metall 27:229–232
69. Reyhani MM, McCormick PG (1994) Effect of thermomechanical cycling in an FeMnSiCrNi shape memory alloy. Scr Metall 31:875–878
70. Bergeon N, Kajiwara S, Kikuchi T (2000) Atomic force microscope study of stress-induced martensite formation and its reverse transformation in a thermomechanically treated Fe-Mn-Si-Cr-Ni alloy. Acta Mater 48:4053–4064
71. Dong ZZ, Kajiwara S, Kikuchi T, Sawaguchi T (2005) Effect of pre-deformation at room temperature on shape memory properties of stainless type Fe-15Mn-5Si-9Cr-5Ni-(0.5-1.5)NbC alloys. Acta Mater 53:4009–4018
72. Wen YH, Zhang W, Li N, Peng HB, Xiong LR (2007) Principle and realization of improving shape memory effect in Fe-Mn-Si-Cr-Ni alloy through aligned precipitations of second-phase particles. Acta Mater 55:6526–6534
73. Lü Y, Hutchinson B, Molodov DA, Gottstein G (2010) Effect of deformation and annealing on the formation and reversion of e-martensite in an Fe-Mn-C alloy. Acta Mater 58:3079–3090
74. Baruj A, Bertolino G, Troiani HE (2010) Temperature dependence of critical stress and pseudoelasticity in a Fe-Mn-Si-Cr pre-rolled alloy". J Alloy Compd 502(1):54–58
75. Stanford N, Dunne DP (2006) Thermo-mechanical processing and shape memory effect in an Fe-based shape memory alloy. Mater Sci Eng A 422(1–2):352–359
76. Baruj A, Troiani HE (2008) The effect of pre-rolling Fe-Mn-Si-based shape memory alloys: mechanical properties and transmission electron microscopy examination. Mater Sci Eng A 481–482:574–577
77. Baruj A, Kikuchi T, Kajiwara S, Shinya N (2004) Improvement of shape memory properties of NbC containing Fe-Mn-Si based shape memory alloys by simple thermomechanical treatments. Mater Sci Eng A 378(1–2):333–336
78. Wen YH, Peng HB, Raabe D, Gutierrez-Urrutia I, Chen J, Du YY (2014) Large recovery strain in Fe-Mn-Si-based shape memory steels obtained by engineering annealing twin boundaries. Nat Commun 5, art. 4964
79. Tanaka Y, Himuro Y, Kainuma R, Sutou Y, Omori T, Ishida K (2010) Ferrous polycrystalline shape-memory alloy showing huge superelasticity. Science 327(5972):1488–1490
80. Omori T, Ando K, Okano M, Xu X, Tanaka Y, Ohnuma I, Kainuma R, Ishida K (2011) Superelastic effect in polycrystalline ferrous alloys. Science 333:68–71
81. Kireeva IV, Chumlyakov YI, Kirillov VA, Karaman I, Cesari E (2011) Orientation and temperature dependence of superelasticity caused by reversible $\gamma$-$\alpha'$ martensitic transformations in FeNiCoAlTa single crystals. Tech Phys Lett 37(5):487–490
82. Sehitoglu H, Karaman I, Zhang XY, Chumlyakov Y, Maier HJ (2011) Deformation of FeNiCoTi shape memory single crystals. Scr Mater 44(5):779–784
83. Sehitoglu H, Zhang XY, Kotil T, Canadinc D, Chumlyakov Y, Maier HJ (2002) Shape memory behavior of FeNiCoTi single and polycrystals. Metall Mater Trans A 33(12):3661–3672
84. Chumlyakov Y, Kireeva IV, Panchenko EY, Zakharova EG, Kirillov VA (2004) Effects of shape memory and superelasticity in FeNiCoTi single crystals with $\gamma \leftrightarrow \alpha$' thermoelastic martensitic transformation. Dokl Phys 394(1):54–57

85. Chumlyakov YI, Kireeva IV, Kretinina IV, Karaman I, Maier H (2013) Shape Memory effect and Superelasticity in the [001] Single crystals of a FeNiCoAlTa Alloy with γ-α′-Thermoelastic Martensitic Transformations. Russ Phys J 56(8):920–929
86. Ma J, Kockar B, Evirgen A, Karaman I, Luo ZP, Chumlyakov Y (2012) Shape memory behavior and tension-compression asymmetry of a FeNiCoAlTa single-crystalline shape memory alloy. Acta Mater 60(5):2186–2195
87. Ma J, Hornbuckle BC, Karaman I, Thompson GB, Luo ZP, Chumlyakov Y (2013) The effect of nanoprecipitates on the superelastic properties of FeNiCoAlTa shape memory alloy single crystals. Acta Mater 61(9):3445–3455
88. Evirgen A, Ma J, Karaman I, Luo ZP, Chumlyakov Y (2012) Effect of aging on the superelastic response of a single crystalline FeNiCoAlTa shape memory alloy. Scr Mater 67(5):475–478
89. Krooß P, Niendorf T, Karaman I, Chumlyakov Y, Maier HJ (2012) Cyclic deformation behavior of aged FeNiCoAlTa single crystals. Funct Mater Lett 5(4):1250045
90. Krooß P, Holzweißig M, Niendorf T, Somsen C, Schaper M, Chumlyakov Y, Maier HJ (2014) Thermal cycling behavior of an aged FeNiCoAlTa single-crystal shape memory alloy. Scr Mater 81:28–31
91. Krooß P, Somsen C, Niendorf T, Schaper M, Karaman I, Chumlyakov Y, Eggeler G, Maier HJ (2014) Cyclic degradation mechanisms in aged FeNiCoAlTa shape memory single crystals. Acta Mater 79:126–137
92. Omori T, Abe S, Tanaka Y, Lee DY, Ishida K, Kainuma R (2013) Thermoelastic martensitic transformation and superelasticity in Fe–Ni–Co–Al–Nb–B polycrystalline alloy. Scr Mater 69:812–815
93. Lee D, Omori T, Kainuma R (2014) Ductility enhancement and superelasticity in Fe–Ni–Co–Al–Ti–B polycrystalline alloy. J Alloy Compd 617:120–123
94. Chumlyakov YI, Kireeva IV, Kutz OA, Kuts OA, Platonova YuN, Poklonov VV, Kukshauzen IV, Kukshauzen DA, Panchenko MYu, Reunova KA (2016) Thermoelastic martensitic transformations in single crystals of FeNiCoAlX(B) alloys. Russ Phys J 58(11):1549–1556
95. Chumlyakov YI, Kireeva IV, Kutz OA, Turabi AS, Karaca HE, Karaman I (2016) Unusual reversible twinning modes and giant superelastic strains in FeNiCoAlNb single crystals. Scr Mater 119:43–46
96. Umino R, Liu XJ, Sutou Y, Wang CP, Ohnuma I, Kainuma R, Ishida K (2006) Experimental determination and thermodynamic calculation of phase equilibria in the Fe-Mn-Al system. JPEDAV 27:54–62
97. Sutou Y, Omori T, Yamauchi K, Ono N, Kainuma R, Ishida K (2005) Effect of grain size and texture on pseudoelasticity in Cu–Al–Mn-based shape memory wire. Acta Mater 53:4121–4133
98. Sutou Y, Omori T, Kainuma R, Ishida K (2013) Grain size dependence of pseudoelasticity in polycrystalline Cu–Al–Mn-based shape memory sheets. Acta Mater 61:3842–3850
99. Chen Y, Schuh CA (2011) Size effects in shape memory alloy microwires. Acta Mater 59:537–553
100. La Roca P, Isola L, Vermaut Ph, Malarria J (2015) Relationship between martensitic plate size and austenitic grain size in martensitic transformations. Appl Phys Lett 106:221903
101. Waitz T, Antretter T, Fischer FD, Simha NK, Karnthaler HP (2007) Size effects on the martensitic phase transformation of NiTi nanograins. J Mech Phys Solids 55:419–444
102. Omori T, Okano M, Kainuma R (2013) Effect of grain size on superelasticity in Fe-Mn-Al-Ni shape memory alloy wire. Appl Phys Lett 1(3):032103
103. Tseng LW, Ma J, Vollmer M, Krooß P, Niendorf T, Karaman I (2016) Effect of grain size on the superelastic response of a FeMnAlNi polycrystalline shape memory alloy. Scr Mater 125:68–72
104. de Castro Bubani F, Sade M, Lovey F (2012) Improvements in the mechanical properties of the 18R ↔ 6R high-hysteresis martensitic transformation by nanoprecipitates in CuZnAl alloys. Mater Sci Eng A 543:88–95
105. Baruj A, Kikuchi T, Kajiwara S, Shinya N (2002) Effect of predeformation of Austenite on shape memory properties in Fe-Mn-Si-based alloys containing Nb and C. Mater Trans 43:585–588
106. Omori T, Nagasako M, Okano M, Endo K, Kainuma R (2012) Microstructure and martensitic transformation in the Fe-Mn-Al-Ni shape memory alloy with B2-type coherent fine particles. Appl Phys Lett 101(23):231907
107. Tseng LW, Ma J, Wang SJ, Karaman I, Kaya M, Lou ZP, Chumlyakov YI (2015) Superelastic response of a single crystalline FeMnAlNi shape memory alloy under tension and compression. Acta Mater 89:234–383
108. Tseng LW, Ma J, Hornbuckle BC, Karaman I, Thompson GB, Lou ZP, Chumlyakov YI (2015) The effect of precipitates on the superelastic response of [011] oriented FeMnAlNi single crystals under compression. Acta Mater 97:234–244
109. Tseng LW, Ma J, Wang SJ, Karaman I, Chumlyakov YI (2016) Effects of crystallographic orientation on the superelastic response of FeMnAlNi single crystals. Scr Mater 116:147–151
110. Vollmer M, Segel C, Krooß P, Günther J, Tseng LW, Karaman I, Weidner A, Biermann H, Niendorf T (2015) On the effect of gamma phase formation on the pseudoelastic performance of polycrystalline Fe-Mn-Al-Ni shape memory alloys. Scr Mater 108:23–26
111. Vollmer M, Krooß P, Kriegel MJ, Klemm V, Somsen C, Ozcan H, Karaman I, Weidner A, Rafaja D, Biermann H, Niendorf T (2016) Cyclic degradation in bamboo-like Fe-Mn-Al-Ni shape memory alloys-The role of grain orientation. Scr Mater 114:156–160
112. Niendorf T, Brenne F, Krooß P, Voller M, Günter J, Schwarze D, Biermann H (2016) Microstructural evolution and functional properties of Fe-Mn-Al-Ni shape memory alloy processed by Selective laser melting. Metall Mater Trans A 47(6):2569–2573
113. Omori T, Iwazako H, Kainuma R (2016) The abnormal grain growth induced by cyclic heat treatment in Fe-Mn-Al-Ni superelastic alloy. Mater Des 101:263–269
114. Duerig TW, Melton KN, Stöckel D, Wayman CM (1990) Engineering aspects of shape memory alloys. Butterworth-Heinemann, London, UK
115. Kajiwara S, Baruj A, Kikuchi T, Shinya N (2003) Low-cost high-quality Fe-based shape memory alloys suitable for pipe joints. Proc SPIE 5053:250–261
116. Otsuka H, Yamada H, Maruyama T, Tanahashi H, Matsuda S, Murakami M (1990) Effects of alloying additions on Fe-Mn-Si shape memory alloys. ISIJ Int 30:674–679
117. Tanahashi H, Maruyama T, Kubo H (1994) Applications of Fe-Mn-Si alloy for pipe joints. Trans Mater Res Soc Jpn 18B:1149–1154
118. Druker AV, Perotti A, Esquivel I, Malarría J (2014) A manufacturing process for shaft and pipe couplings of Fe-Mn-Si-Ni-Cr shape memory alloys. Mater Des 56:878–888
119. Druker AV, Perotti A, Esquivel I, Malarría J (2014) Optimization of Fe-15Mn-5Si-9Cr-5Ni shape memory alloy for pipe and shaft couplings. J Mater Eng Perform 23:2732–2737
120. Watanabe Y, Miyazaki E, Okada H (2002) Enhanced mechanical properties of Fe-Mn-Si-Cr shape memory fiber/plaster smart composite. Mater Trans 43(5):974–983

121. Mino J, Komanicky V, Durisin M, Sakl K, Kovac J, Varga R (2015) Structural and magnetic characterization of Fe-Mn-Al-Ni Pseudo-Heusler alloy. IEEE Trans Magn 51(1):4000903
122. Grässel O, Krüger L, Frommeyer G (2000) L.W Meyer: High strength Fe-Mn-(Al, Si) TRIP/TWIP steels development—properties—application. Int J Plast 16(10–11):1391–1409
123. Nikulin I, Sawaguchi T, Tsuzaki K (2013) Effect of alloying composition on low-cycle fatigue properties and microstructure of Fe-30Mn-(6x)Si-xAl TRIP/TWIP alloys". Mater Sci Eng A 587:192
124. Millán J, Sandlobes S, Al-Zubi A, Hickel T, Choi P, Neugebauer J, Ponge D, Raabe D (2014) Designing Heusler nanoprecipitates by elastic misfit stabilization in Fe-Mn maraging steels. Acta Mater 76:94–105
125. Cladera A, Weber B, Leinenbach C, Czaderski C, Shahverdi M, Motavalli M (2014) Iron-based shape memory alloys for civil engineering structures: an overview. Constr Build Mater 63:281
126. Sawaguchi T, Sahu P, Kikuchi T, Ogawa K, Kajiwara S, Kushibe A, Higashino M, Ogawa T (2006) Vibration mitigation by the reversible fcc/hcp martensitic transformation during cyclic tension compression loading of an Fe-Mn-Si-based shape memory alloy. Scr Mater 54:1885
127. Sawaguchi T, Bujoreanu L-G, Kikuchi T, Ogawa K, Koyama M, Murakami M (2008) Mechanism of reversible transformation-induced plasticity of Fe-Mn-Si shape memory alloys. Scr Mater 59:826
128. Sawaguchi T, Nikulin I, Ogawa K, Sekido K, Takamori S, Maruyama T, Chiba Y, Kushibe A, Inouec Y, Tsuzaki K (2015) Designing Fe-Mn-Si alloys with improved low-cycle fatigue lives". Scr Mater 99:49–52
129. Jani JM, Leary M, Subic A, Gibson MA (2014) A review of shape memory alloy research, applications and opportunities. Mater Des 56:1078–1113